Temperature-Programmed Desorption Investigation of the Adsorption and Reaction of Butene Isomers on Pt(111) and Ordered Pt–Sn Surface Alloys

ARTICLE · APRIL 1997

DOI: 10.1021/jp9638245

Temperature-Programmed Desorption Investigation of the Adsorption and Reaction of Butene Isomers on Pt(111) and Ordered Pt−Sn Surface Alloys

Yi-Li Tsai and Bruce E. Koel*

Department of Chemistry, University of Southern California, Los Angeles, California 90089-0482

Received: November 15, 1996; In Final Form: January 6, 1997[⊗]

The influence of alloyed Sn on the chemistry of C_4 butene isomers, including 1-butene, *cis*-2-butene, and isobutene, chemisorbed on Pt(111) was investigated by temperature-programmed desorption (TPD), Auger electron spectroscopy (AES), and low-energy electron diffraction (LEED). Pt−Sn alloy chemistry was probed by investigation of two ordered surface alloys formed when Sn atoms were incorporated within the topmost layer on a Pt(111) substrate to form a (2 × 2) Sn/Pt(111) alloy with $\Theta_{Sn} = 0.25$ and a ($\sqrt{3} \times \sqrt{3}$)R30° Sn/Pt(111) alloy with $\Theta_{Sn} = 0.33$. Low-coverage states of chemisorbed 1-butene, *cis*-2-butene, and isobutene on Pt(111) have desorption activation energies of 17.5, 17, and 17 kcal/mol, respectively. These energies are reduced to 16, 15.5, and 15 kcal/mol on the (2 × 2) alloy and 13.5, 12, and 11 kcal/mol on the ($\sqrt{3} \times \sqrt{3}$)R30° alloy. Changing the surface Sn concentration from $\Theta_{Sn} = 0.25$ to $\Theta_{Sn} = 0.33$ causes a relatively larger decrease in the chemisorption bond strength of these alkenes, and we associate this with the importance of a pure Pt 3-fold site for strong alkene bonding. All three butenes undergo decomposition on Pt(111) during TPD which accounts for 50−60% of the chemisorbed monolayer. Alloying Sn into the surface causes a large reduction in the reactivity of the surface, and the fraction of the chemisorbed layer which decomposes is decreased to 3−7% on the (2 × 2) alloy, and no decomposition occurs on the ($\sqrt{3} \times \sqrt{3}$)R30° alloy. The strong reduction of decomposition on these two surface alloys may be due to the elimination of adjacent pure Pt 3-fold hollow sites. No large changes occur in the coverage of the chemisorbed monolayer of butenes in the presence of up to 33% of a monolayer of alloyed Sn, showing that the adsorption ensemble requirement for chemisorption of these alkenes on Pt(111) and the two Sn/Pt(111) alloys is at most a few Pt atoms. To the extent that alloying or direct Pt−Sn interactions occur in supported, bimetallic Pt−Sn catalysts, the chemistry reported here would lead to increased isobutene yields and decreased coking of the catalyst.

1. Introduction

We are investigating the chemistry of a series of hydrocarbons on ordered Pt−Sn surface alloys that can serve as models of supported bimetallic Pt−Sn heterogeneous catalysts. Generally, the addition of Sn to Pt catalysts for hydrocarbon conversion decreases the catalytic activity but increases the selectivity for unsaturated hydrocarbon products and reduces coking, thus prolonging the lifetime of the catalyst. The role of Pt−Sn alloy phases in this chemistry is a subject of debate, and there is minimal fundamental underpinning of this discussion from surface science since so little is known about the chemisorption and reaction of hydrocarbons on well-defined Pt−Sn alloy surfaces. In addition, the catalytic dehydrogenation of butane and isobutane to isobutene is of particular interest since isobutene is important as a source of MTBE, a gasoline additive. In order to provide some fundamental information on this reaction over metal surfaces, we have investigated the adsorption and reaction of butane and isobutane,[1] H_2,[2] and now butene isomers on the Pt(111) surface and on two ordered Pt−Sn surface alloys.

Extensive work on olefinic molecule adsorption has been carried out previously on transition metals, especially on Pt(111). Ethylene,[3−11] propylene,[4,8,12−15] and all of the butene (C_4) isomers[4,8,12,16,17] are di-σ-bonded to Pt(111) at low temperatures (95−260 K). The molecular adsorbates desorb or transform into alkylidyne surface species near room temperature. In particular, Cassuto and Tourillon[16] showed using near-edge X-ray adsorption fine structure (NEXAFS) and ultraviolet photoelectron spectroscopy (UPS) that all four butene isomers on Pt(111) had identical adsorption geometries, i.e., di-σ-bonded with the chemisorbed C−C bond parallel to the Pt surface plane, and similar chemisorption bond strengths (peak desorption temperatures of 260−280 K).

In this paper, TPD is primarily used to extend information on the adsorption, desorption, and dehydrogenation of several butene isomers (1-butene, *cis*-2-butene, and isobutene) on Pt(111) and to provide the first results for butenes adsorbed on two well-defined Pt−Sn surface alloys—the (2 × 2) and ($\sqrt{3} \times \sqrt{3}$)R30° Sn/Pt(111) alloys. In particular, we determine the influence of alloyed Sn on the chemistry of these molecules. In this paper, we have not studied the adsorption and reaction of *trans*-2-butene, since the results for *cis*- and *trans*-2-butene on Pt(111) were reported to be very similar using TPD measurements.[4]

2. Experimental Methods

These experiments were performed in a stainless steel UHV chamber pumped by a 220 L/s ion pump, Ti sublimation pump, and 170 L/s turbomolecular pump. The base pressure was kept at 1×10^{-10} Torr during the experiments. The chamber was equipped with a double-pass cylindrical mirror analyzer (CMA) for AES, a four-grid electron optics for LEED, a UTI 100 C quadrupole mass spectrometer (QMS) for TPD, an ion gun for Ar^+ ion sputtering, and directed beam microcapillary dosers for gas exposures.

The Pt(111) single-crystal sample (Atomergic, 5 N purity) was 10 mm in diameter and 1 mm thick. A detailed description of the sample holder including the heating and cooling setup was reported previously.[18] We were able to achieve a substrate

[⊗] Abstract published in *Advance ACS Abstracts,* February 15, 1997.

S1089-5647(96)03824-2 CCC: $14.00

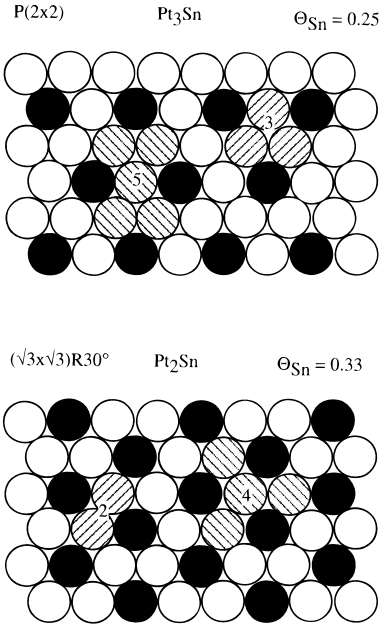

Figure 1. Schematic diagram of the structure of two Sn/Pt(111) surface alloys. Top: Top view of the (2 × 2) Sn/Pt(111) surface alloy. Bottom: Top view of the ($\sqrt{3} \times \sqrt{3}$)R30°Sn/Pt(111) surface alloy. Several small ensembles of contiguous Pt atom clusters are cross-hatched and identified by the number of Pt atoms in the ensemble.

temperature from 90 to 1200 K using this design, as measured by a chromel−alumel thermocouple spotwelded to the side of the crystal. The Pt(111) crystal was cleaned by a standard procedure of Ar^+ ion sputtering, heating in oxygen, and annealing in vacuum.[18] The cleanliness of the surface was checked by AES and LEED before the experiments. TPD measurements were taken with the crystal surface in line of sight to the QMS ionizer and using a linear heating rate of 4 K s^{-1}. We also utilized a stainless steel shield for the QMS to eliminate the electron flux from the ionizer and attenuate background gas contributions as described elsewhere.[19] In the TPD experiments, we monitored signals at 2, 15, 16, 28, 30, 38, 40, 42, 44, 54, 56, 58, and 78 amu.

The gases 1-butene (Aldrich, 99% purity), *cis*-2-butene (Aldrich, 97.7% with the major impurity as *trans*-2-butene), and isobutene (Aldrich, 99%) were used from the lecture bottles without further purification. The purity was monitored in situ by mass spectroscopy. Gas exposures were carried out via a leak valve connected to a microcapillary array doser, which was about 10 mm in front of the Pt(111) single crystal. All exposures were made with the crystal at 95 K. Gas exposures in this paper are given in units of langmuir (1 langmuir = 10^{-6} Torr·s). We calculated the factors for the doser enhancement in flux and ion gauge sensitivity correction by using uptake curves along with the knowledge that the sticking (condensation) coefficient is unity[19,20] for the butenes on Pt(111) at 95 K (the coverage scale can be set by TPD, as we will show below). The coverages used throughout this paper are referenced to the Pt(111) surface atom density of 1.505 × 10^{15} atoms cm^{-2}, corresponding to Θ = 1.0 ML (ML = monolayer).

Two ordered Pt−Sn surface alloys can be prepared by evaporating Sn at different coverages on Pt(111) at 300 K and then annealing to 1000 K for 10 s.[21] LEED shows two structures, either a (2 × 2) or ($\sqrt{3} \times \sqrt{3}$)R30° pattern. Both of these surfaces correspond to substitutional alloys, as shown in Figure 1, in which the Sn atoms sit only 0.2 Å above the plane of the first layer Pt atoms.[22] The structure of these surfaces has also been confirmed by LEED I−V analysis[23] and X-ray photoelectron diffraction (XPD).[24] These alloys have the stoichiometry

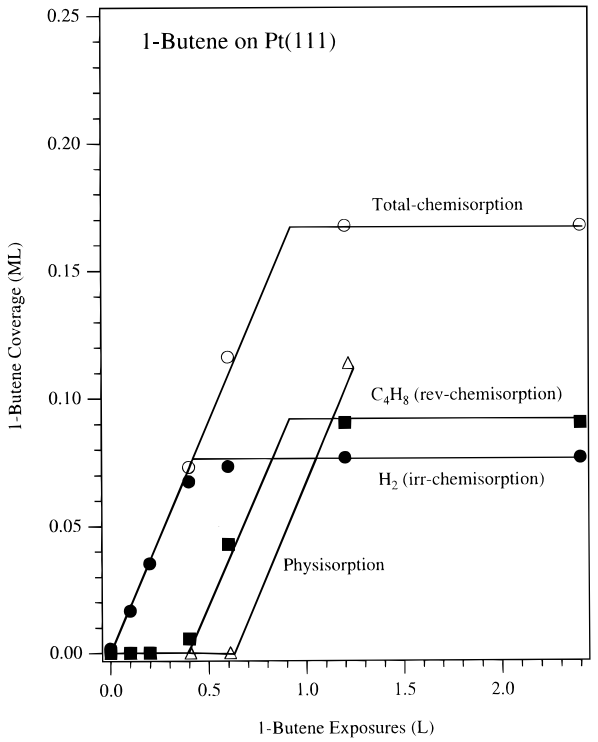

Figure 2. Uptake curve that results from TPD experiments for 1-butene adsorption on Pt(111) at 95 K.

of either Pt_3Sn with Θ_{Sn} = 0.25 or Pt_2Sn with Θ_{Sn} = 0.33 in the surface layer. For convenience, the (2 × 2) Sn/Pt(111) and ($\sqrt{3} \times \sqrt{3}$)R30°Sn/Pt(111) surface alloys will be referred to as the (2 × 2) and $\sqrt{3}$ alloys, respectively, throughout this paper. These ordered alloys constrain the Pt ensemble size (number of contiguous reactive Pt atoms as marked in Figure 1) available for adsorption and reaction to rather small numbers (five for the (2 × 2) and four Pt atoms for the $\sqrt{3}$ alloy) and also allow fine control of the reactive sites available at the surface. For the (2 × 2) alloy, pure Pt 3-fold hollow sites are present but no adjacent pure Pt 3-fold sites. For the $\sqrt{3}$ alloy, all 3-fold Pt sites are eliminated and the distance between adjacent pure Pt 2-fold bridge sites is increased.

3. Results

3.1. 1-Butene. Figure 2 summarizes the adsorption kinetics of 1-butene on Pt(111) obtained from TPD measurements following various 1-butene exposures at 95 K. H_2 and C_4H_8 were the only gases observed desorbing from the surface. There are two goals to construct the uptake curves: first, to evaluate the amount of adsorbed 1-butene that decomposes during TPD and, second, to determine the saturation coverage of 1-butene chemisorption. The procedure for calibration of the uptake curve is reported in slightly more detail elsewhere.[19] Briefly, we utilize the H_2 TPD area from the well-known decomposition of ethylene on Pt(111) to give an absolute calibration for the hydrogen yield from the irreversibly adsorbed 1-butene coverage simply by using stoichiometry. Since the sticking coefficient for 1-butene on Pt(111) at 95 K is unity,[20] independent of coverage, we calibrate the C_4H_8 TPD area reflecting the reversibly adsorbed 1-butene coverage by forcing the slope of the 1-butene uptake curve to be the same as that for the irreversibly adsorbed curve under conditions that the H_2 TPD yield is constant. The saturation coverage of the 1-butene chemisorption monolayer is given by the sum of the two curves, irreversibly and reversibly adsorbed 1-butene, i.e., the amounts of H_2 and 1-butene desorption, respectively. On Pt(111), the

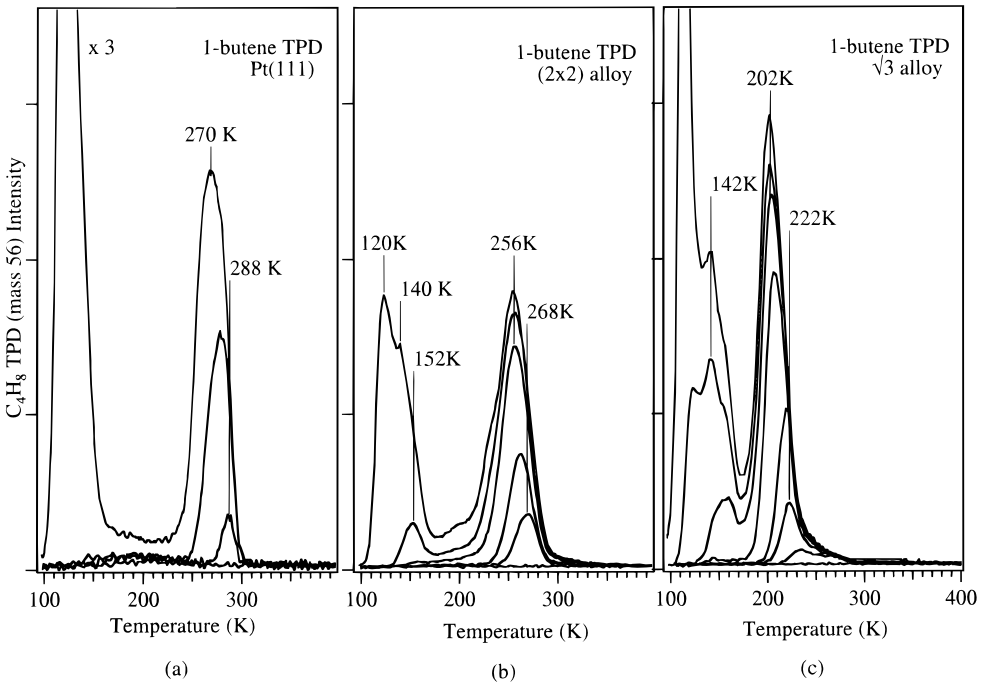

Figure 3. (a) C_4H_8 TPD spectra following 1-butene exposures on Pt(111) at 95 K. The exposures were 0.20, 0.40, 0.60, and 1.2 langmuir of 1-butene. (b) C_4H_8 TPD spectra after 1-butene exposures on the (2 × 2) alloy at 95 K. The exposures were 0.0, 0.10, 0.20, 0.40, 0.60, and 1.2 langmuir of 1-butene. (c) C_4H_8 TPD spectra following 1-butene exposures on the $\sqrt{3}$ alloy at 95 K. The exposures were 0.0, 0.04, 0.10, 0.20, 0.40, 0.60, 1.2, and 2.0 langmuir of 1-butene.

saturation coverage of 1-butene in the chemisorbed monolayer is 0.17 ML. During TPD, 0.08 ML of 1-butene decomposes and 0.09 ML desorbs molecularly as 1-butene. Physisorption to form condensed multilayers occurs at larger exposures, and the initial population of these states is also shown in Figure 2. We also used AES to monitor the amount of residual carbon on the surface after each TPD spectrum for this case and all of the others. The extent of butene decomposition determined in this manner gave values consistent with those obtained from the uptake curves, as will be discussed later.

Figure 3a shows a series of 1-butene (C_4H_8, mass 56) TPD spectra after 1-butene adsorption on Pt(111) at 95 K for increasing 1-butene exposures.[25] For exposures of less than 0.20 langmuir, all of the chemisorbed 1-butene is irreversibly adsorbed and no molecular desorption occurs. Chemisorbed 1-butene initially desorbs in a peak at 288 K. We roughly estimate that this corresponds to a desorption activation energy of 17.5 kcal/mol. In this paper, all of the conversions from desorption peak temperatures to desorption activation energies used Redhead analysis[26] with an assumption of first-order desorption kinetics and a preexponential factor of 10^{13} s^{-1}, and we quote desorption activation energies to the nearest 0.5 kcal/mol. The peak desorption temperature of reversibly chemisorbed 1-butene decreases as the 1-butene exposure increases. It moves from 288 to 270 K at 1 monolayer coverage of 1-butene. The corresponding activation energy for the peak at 270 K is 16.5 kcal/mol. The shift of desorption peak toward lower temperatures with increasing coverages in the monolayer was seen for all of the butene isomers studied on these three surfaces. It is likely due to a decrease in the heat of adsorption from lateral repulsive interactions between chemisorbed molecules in the monolayer. Higher exposures of 1-butene produce physisorbed molecules that desorb in a peak at 120 K. A high-temperature shoulder on the multilayer desorption peak on Pt(111) modifies the peak shape from the typical zeroth-order desorption profile that is characterized by a instantaneous drop in peak intensity after the peak maximum. This shoulder corresponds to a weakly bonded state at about 140 K. This weakly bonded state is seen more clearly in Figure 3b and 3c and was seen for all of the butene isomers on all of the surfaces studied.

Figure 3b shows the TPD spectra of 1-butene desorption for increasing exposures of 1-butene on the (2 × 2) alloy at 95 K. Reversibly adsorbed 1-butene occurs at exposures as low as 0.10 langmuir, compared to about 0.40 langmuir on the Pt(111) surface. Chemisorbed 1-butene desorbs in a peak at 268 K at low coverage, and the peak temperature shifts to 256 K at monolayer coverage. The corresponding activation energies are 16.5 and 15.5 kcal/mol, respectively. After saturating the monolayer, further exposures form a weakly bonded state that desorbs initially in a peak at 152 K, and this shifts to about 140 K at larger coverages. In addition, a physisorbed multilayer peak was observed at 120 K, and this lowest temperature peak could be increased in size with no limit with larger exposures.

A series of 1-butene TPD spectra for increasing 1-butene exposures on the $\sqrt{3}$ alloy at 95 K are shown in Figure 3c. Chemisorbed 1-butene desorbs at 222−202 K depending on the coverage in the monolayer, with corresponding activation energies of 13.5 and 12.0 kcal/mol, respectively. Prior to the formation of the multilayer desorption peak, a sharp peak at 114 K, other features appear with desorption peak temperatures of 155 and 142 K.

Figure 4 compares the molecular 1-butene desorption spectra on all three surfaces. An exposure of 1.2 langmuir of 1-butene was used which saturates the chemisorbed monolayer and produces some physisorbed species. The desorption temperature of the chemisorbed 1-butene shifts down as the surface Sn concentration goes up. At monolayer coverage, the peak temperature decreases from 270 K on Pt(111) to 256 K on the (2 × 2) alloy and further to 202 K on the $\sqrt{3}$ alloy. On Pt(111), the amount of 1-butene molecular desorption is smaller than that from the two surface alloys even though similar monolayer coverages of 1-butene are formed on all of these substrates (as we will discuss later in Table 1). This must mean that less decomposition occurs on alloys during TPD, and this is shown

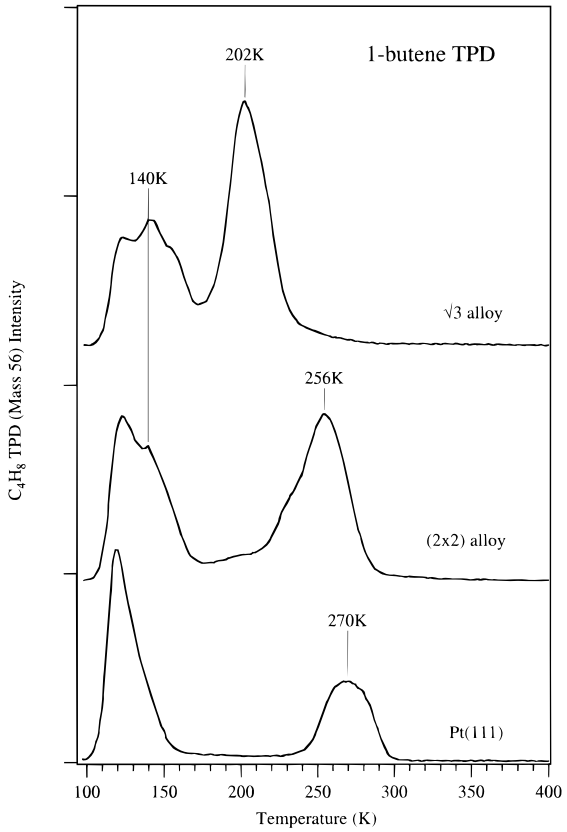

Figure 4. Comparison of the C_4H_8 TPD spectra after 1.2-langmuir 1-butene exposures on all three surfaces at 95 K to produce a chemisorbed monolayer and some concentration of physisorbed species.

clearly below. Alloyed Sn weakens the bonding of 1-butene to the surface and suppresses the decomposition of chemisorbed 1-butene.

Although we have not yet carried out surface vibrational spectroscopy to investigate the bonding of 1-butene on the Sn/Pt(111) surface alloys, we have some insight into this issue from our previous high-resolution electron-energy-loss spectroscopy (HREELS) studies of ethylene bonding on these Sn/Pt(111) surface alloys.[27] These studies showed that ethylene was di-σ-bonded on both alloy surfaces but that ethylene was less rehybridized toward sp^3 as the Sn concentration increased. Our observation of a similar decrease in the desorption activation energy, i.e., weakening of the chemisorption bond strength, of 1-butene on the surface alloys compared to that for ethylene strongly suggests that di-σ-bonded 1-butene is the surface species formed on these two surface alloys at low temperature.

Obviously, it is difficult to assign the origin of the weakly bonded states that desorb from all three surfaces at 140−155 K. These peaks could be due to a species in the chemisorbed monolayer weakly π-bonded to the surface or a species in the second layer (that would also have a C═C double bond and thus π-bonding within the molecule). Aided by a quantitative analysis of the 1-butene TPD spectra, these low-temperature peaks (140−155 K) and the strongly bound peaks (200−290 K) have similar areas and so have similar coverages. Thus, we favor an assignment of this weakly bonded state to species that are not part of the chemisorbed monolayer, i.e., not forming site-specific and geometry-specific bonding interactions with the surface, but that do have a fair energetic distinction from the formation of the multilayer state on these surfaces due to some appreciable interaction with the surface. This observation and assignment is discussed in a bit more detail with reference to isobutene desorption in another paper.[19]

The H_2 TPD spectra following various exposures of 1-butene on Pt(111) at 95 K are shown in Figure 5a. The H_2 yield was a constant for all exposures $\geq$0.40 langmuir. This is consistent with the molecular 1-butene desorption shown in Figure 3a, where the reversibly adsorbed 1-butene starts to form at an exposure near 0.40 langmuir. At low 1-butene coverage (0.10-langmuir exposure), H_2 desorption occurs in a peak at 345 K with a shoulder at 400 K. H_2 desorption from H_2 exposures[2] is at a similar temperature of 350 K, and this indicates that H_2 desorption from decomposition of low coverages of 1-butene on Pt(111) is H_2-desorption rate-limited. At monolayer coverage of 1-butene, the H_2 desorption profile has a lot of structure with three groups of peaks located at 250−330 and 330−480 K and a broad peak centered at 620 K.

In Figure 5b, we show the C_4H_x stoichiometry for the species formed from sequential dehydrogenation of the 1-butene monolayer on Pt(111) as a function of the crystal temperature using the H_2 TPD spectra for monolayer coverage. The C_4H_x stoichiometry comes from an integration of the H_2 desorption peak areas on Pt(111) following a normalization of the mass spectrometer intensity to remove the influence of the surface temperature on the H_2 sensitivity (ref 19 and references cited therein). We confirm the assignment of Avery and Sheppard [8] that the H_2 desorption peak at 296 K is due to the formation of butylidyne (C_4H_7), where each irreversibly chemisorbed 1-butene molecule (C_4H_8) releases one H. These authors[8] also used HREELS to show that butylidyne is formed at room temperature. The H_2 desorption peaks with temperatures between 326 and 480 K, shown in Figure 5a, correspond in total to the liberation of 4.5 H/molecule. The overall stoichiometry of all surface species at 480 K is hence $C_4H_{2.5}$. This result is slightly different from the value of C_4H_2 reported previously.[8] Noninteger stoichiometry is certainly possible for the surface species since several different fragments can coexist on the surface, e.g., C_2H + CH, etc. Carbon−carbon bond-breaking reactions have been proposed to occur at a temperature near 500 K.[8] In summary, the H_2 desorption ratios for 1-butene on Pt(111) are 1:4.5:2.5, corresponding to the three regions in Figure 5a. Schematically, we can write the following dehydrogenation mechanism:

$$C_4H_8 \xrightarrow{296\ K} C_4H_7 \xrightarrow{408\ K} C_4H_{2.5}$$

H_2 desorption spectra from 1-butene monolayers on Pt(111) and the (2 × 2) and $\sqrt{3}$ surface alloys are shown in Figure 6a. The amount of H_2 evolution from the (2 × 2) alloy is only 14% of the H_2 yield from Pt(111), and this corresponds to a decomposition of 7% of the chemisorbed 1-butene on the (2 × 2) alloy. No H_2 desorption was detected from the $\sqrt{3}$ alloy. Alloyed Sn dramatically suppresses the decomposition (as monitored by the H_2 desorption) of chemisorbed 1-butene from both alloys, even though similar chemisorption coverages were obtained on all of these three surfaces. AES measurements taken after TPD on both surface alloys are consistent with these H_2 TPD results that only a small amount of or no decomposition occurs on the (2 × 2) and $\sqrt{3}$ alloys.

Figure 6b shows H_2 TPD spectra from increasing 1-butene exposures on the (2 × 2) alloy. A fairly sharp peak near 410 K and a broad peak with a maximum at 670 K were observed for all exposures. The H_2 desorption peaks below 300 K are due to cracking fractions of desorbed 1-butene in the QMS ionizer. The main peak at 410 K is very close to the temperature of the main H_2 peak on Pt(111) due to butylidyne decomposition, and it is possible that butylidyne formation occurs on this surface, too. The H_2 evolution from initial dehydrogenation of 1-butene (possibly to form butylidyne) appears as a shoulder

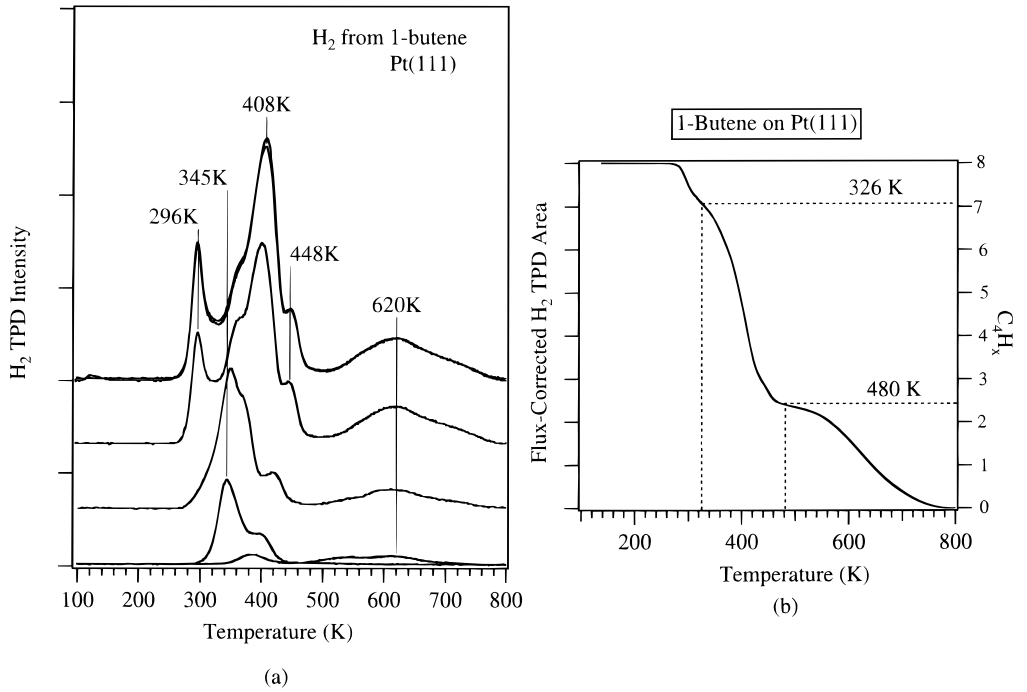

Figure 5. (a) H_2 desorption resulting from 1-butene decomposition on Pt(111). The exposures were 0.0, 0.10, 0.20, 0.40, 0.60, and 1.2 langmuir of 1-butene on Pt(111) at 95 K. (b) Surface stoichiometry of hydrocarbon fragments resulting from the dehydrogenation of the 1-butene (C_4H_8) monolayer as a function of temperature on Pt(111).

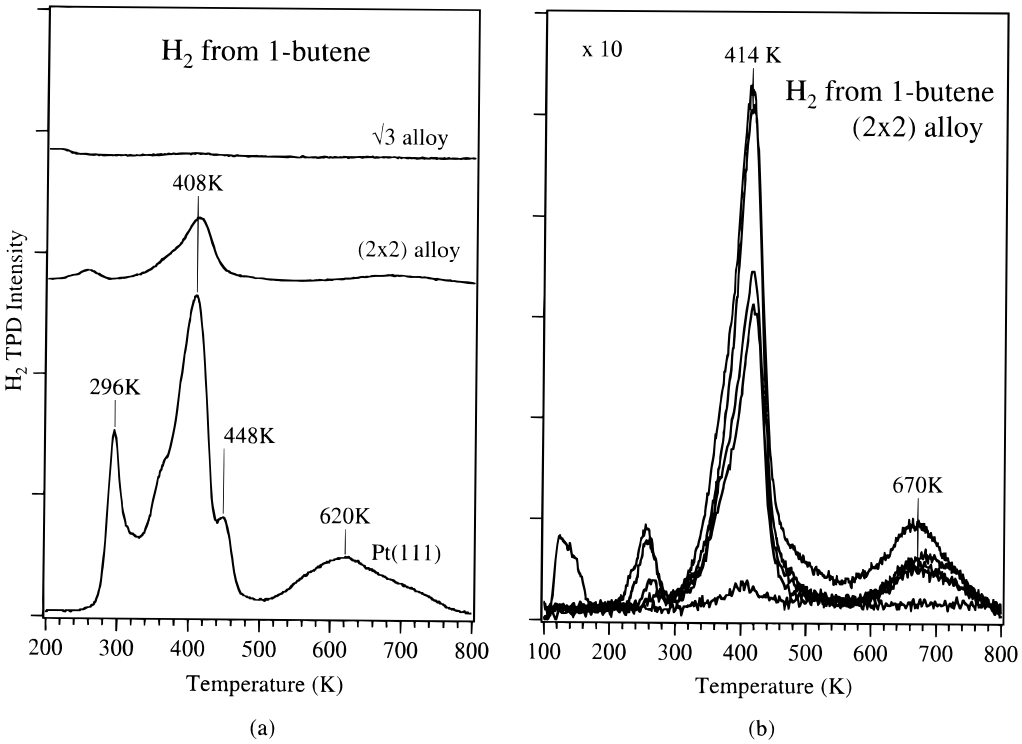

Figure 6. (a) Comparison of the H_2 desorption spectra from 1-butene decomposition on Pt(111), the (2 × 2) and $\sqrt{3}$ alloy surfaces. (a) H_2 desorption from 1-butene decomposition on the (2 × 2) alloy. The exposures were 0.0, 0.20, 0.40, 0.60, and 1.2 langmuir of 1-butene on the (2 × 2) alloy at 95 K.

on the low-temperature leading edge of this peak. H_2 desorption from atomic H dosed to the (2 × 2) alloy surface occurs at 337−371 K,[28] so it is not clear whether or not this H_2 evolution is H_2-desorption rate-limited or reaction-rate-limited. The first step in the butylidyne decomposition mechanism on the (2 × 2) alloy and the corresponding activation energy appears to be quite similar to that on Pt(111) since the H_2 evolution has a similar peak temperature and profile. Differences occur in the higher temperature region where the peaks at 448 and 620 K on Pt(111) are absent on the (2 × 2) alloy, indicating a different butylidyne decomposition mechanism.

While it is tempting to assign the small H_2 evolution on the (2 × 2) alloy to defective Pt(111)-like regions and we cannot rule out a very small concentration of such defects, it is quite likely that these results reflect appropriately the alkene chemistry of the nondefective alloy. We make this conclusion for several reasons. First, alkane thermal desorption occurs in narrow peaks characteristic of Pt(111) or the alloy surface,[1] and these results

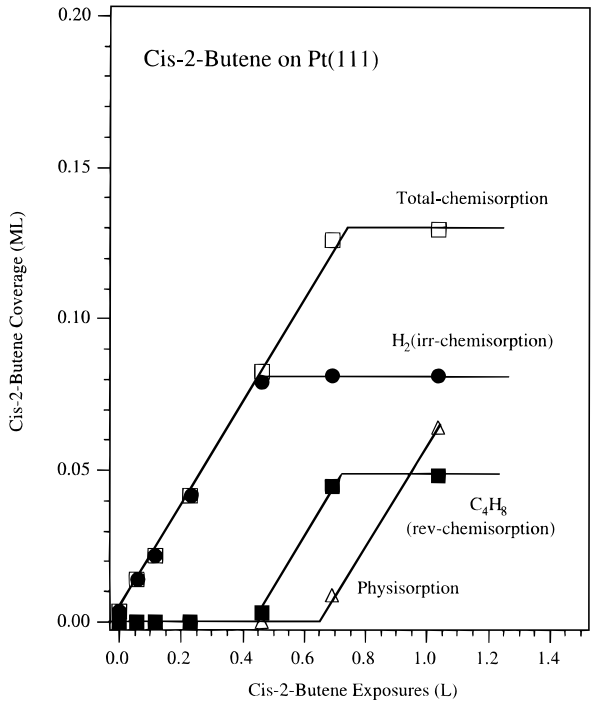

Figure 7. Uptake curve that results from TPD experiments for *cis*-2-butene adsorption on Pt(111) at 95 K.

show clearly that Pt(111)-like defects are below 1% on the (2 × 2) alloys prepared properly. Second, the H_2 evolution from the low background exposures shown in Figures 5a and 6a occurs at different temperatures, which would not be expected if Pt(111)-like defects had any significant concentration on the alloy surface. Finally, low coverages of butylidyne on Pt(111) thermally decomposes to give quite a different H_2 TPD spectrum.

No ordered structures due to an adsorbate lattice were observed by LEED following 1-butene adsorption on either alloy surface at 95 K. A number of annealing experiments at various temperatures were carried out carefully following the formation of a multilayer coverage of 1-butene on the (2 × 2) and $\sqrt{3}$ alloys, and no extra spots in addition to the alloy structures were seen by LEED.

3.2. *cis*-2-Butene. The adsorption of *cis*-2-butene on Pt(111) at 95 K is described by the uptake curves shown in Figure 7. These curves are constructed from the H_2 and *cis*-2-butene TPD spectra (shown below) and are denoted as irreversible and reversible adsorption, respectively. The calibration procedure used was identical to that presented above for 1-butene. For *cis*-2-butene on Pt(111), the coverage for the chemisorbed monolayer is 0.13 ML, with 0.08 ML irreversibly adsorbed and 0.05 ML reversibly adsorbed. Additional uptake at higher exposures due to the formation of physisorbed species is also shown in Figure 7.

TPD spectra for C_4H_8 after increasing *cis*-2-butene exposures on Pt(111) at 95 K are given in Figure 8a. At low coverage (<0.24 langmuir), all of the chemisorbed *cis*-2-butene is irreversibly adsorbed. Thus, H_2 is liberated from the surface and no molecular desorption is detected during TPD. The desorption peak from reversibly chemisorbed *cis*-2-butene occurs initially at 270 K after 0.48-langmuir *cis*-2-butene exposure and then shifts to 260 K at monolayer coverage. An exposure of 0.71 langmuir of *cis*-2-butene on Pt(111) at 95 K forms both the strongly chemisorbed state and a weakly bonded state that gives rise to a peak at 142 K. An exposure of 1.1 langmuir produces a multilayer peak at 130 K, and this peak could be increased in size indefinitely with larger exposures. As with 1-butene, repulsive interactions also exist within the *cis*-2-butene chemisorbed monolayer. This reduces the desorption peak temperature from 270 to 260 K and the corresponding activation energies for desorption from 16.5 to 16.0 kcal/mol with increasing *cis*-2-butene coverage.

TPD spectra for *cis*-2-butene for increasing *cis*-2-butene exposures on the (2 × 2) alloy at 95 K are given in Figure 8b. C_4H_8 desorption from a chemisorbed state is initially observed in a peak at 254 K after exposures as low as 0.06 langmuir. This indicates that reversible adsorption of *cis*-2-butene occurs on the (2 × 2) alloy even at low coverages, in contrast to the chemistry seen on Pt(111). At monolayer coverage, the desorption peak of chemisorbed *cis*-2-butene is very broad, extending to lower temperatures and shifting the peak to 222 K. The desorption activation energies corresponding to peaks at 254 and 222 K are 15.5 and 13.0 kcal/mol, respectively. At higher exposures, *cis*-2-butene forms a weakly bonded state that is desorbed at 150 K and a multilayer state that desorbs initially in a peak at 130 K.

A series of C_4H_8 TPD spectra for increasing *cis*-2-butene exposures on the $\sqrt{3}$ alloy at 95 K are shown in Figure 8c. The C_4H_8 desorption peak for reversibly chemisorbed species shifts from 200 to 176 K as the exposure increases from 0.12 to 0.71 langmuir. A clearly distinguishable peak at 152 K was observed following 1.1-langmuir exposure. Multilayer desorption gives rise to a peak at 124 K after *cis*-2-butene exposures of ≥1.1 langmuir on the $\sqrt{3}$ alloy.

Figure 9 compares molecular desorption for monolayer coverages of *cis*-2-butene on these substrates. Alloyed Sn weakens the chemisorption bond strength as can be seen in the decreased desorption temperature with increasing Sn concentration. Surface Sn atoms in the alloys also suppress *cis*-2-butene decomposition, since the *cis*-2-butene desorption yields from both alloys are larger than that from Pt(111) and very similar monolayer coverages are observed for all of these three surfaces (about 0.13 ML as will be shown in Table 1). This figure also shows that a weakly bonded state that desorbs near 150 K occurs on all three surfaces. The assignment of the origin of this peak is not clear, but we currently do not favor attributing it to the chemisorbed monolayer as a π-bonded chemisorbed species.

H_2 TPD from the decomposition of chemisorbed *cis*-2-butene on Pt(111) is shown in Figure 10a. H_2 desorption from *cis*-2-butene exposures of ≤0.24 langmuir forms a sharp peak at 352 K, which is H_2-desorption rate-limited on Pt(111), and a broad peak extending to 800 K. Consistent with our results for molecular *cis*-2-butene desorption, the H_2 TPD yield, and thus the amount of irreversible adsorption, is saturated by 0.48-langmuir *cis*-2-butene exposure. The H_2 TPD spectrum from near monolayer coverages of *cis*-2-butene is comprised of peaks at 302 and 384 K and a broad peak centered at 610 K. In Figure 10b, we take this top H_2 TPD spectrum and integrate to determine the amount of H_2 desorption as a function of temperature after making a flux correction. This graph also shows on the right-hand side the overall stoichiometry (C_4H_x) of the surface species formed from thermal decomposition of a monolayer coverage of *cis*-2-butene on Pt(111). One sees that the H_2 desorption ratios are 1.6:4.2:2.2 for the peaks at 302, 384, and 610 K. A general schematic diagram for *cis*-2-butene dehydrogenation on Pt(111) is as follows:

$$C_4H_8 \xrightarrow{302\ K} C_4H_{6.4} \xrightarrow{384\ K} C_4H_{2.2}$$

We interpret these results to be almost the same as those for 1-butene, with the formation of butylidyne by losing one

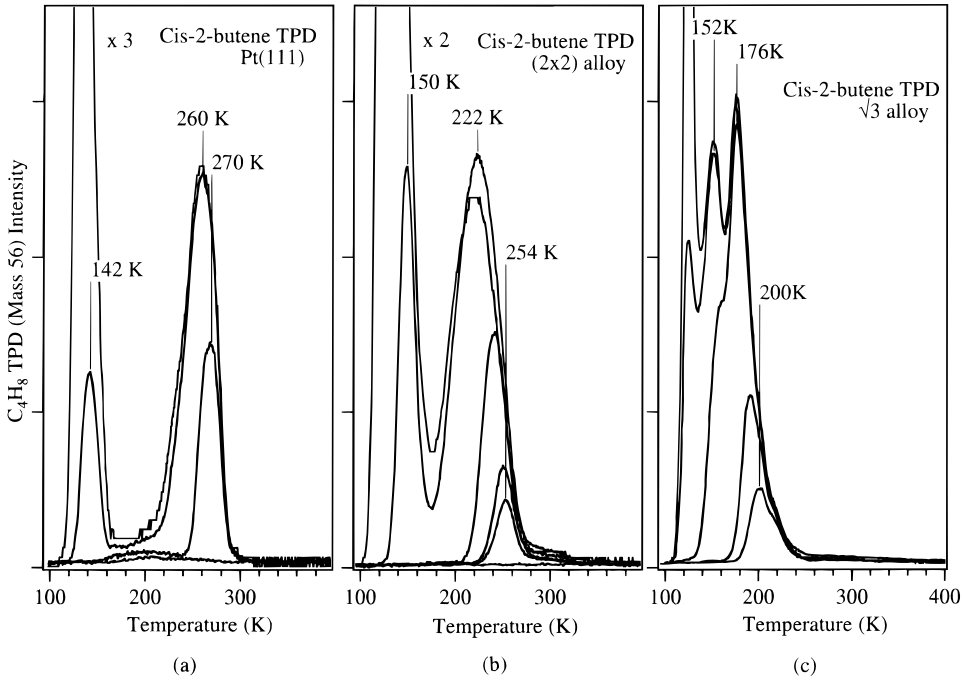

Figure 8. (a) C_4H_8 TPD spectra from *cis*-2-butene exposures on Pt(111) at 95 K. The exposures were 0.24, 0.48, 0.71, and 1.1 langmuir of *cis*-2-butene. (b) C_4H_8 TPD spectra from *cis*-2-butene exposures on the (2 × 2) alloy at 95 K. The exposures were 0.0, 0.06, 0.12, 0.24, 0.71, and 1.4 langmuir of *cis*-2-butene. (c) C_4H_8 TPD spectra from *cis*-2-butene exposures on the $\sqrt{3}$ alloy at 95 K. The exposures were 0.12, 0.24, 0.71, 1.1, and 1.4 langmuir of *cis*-2-butene.

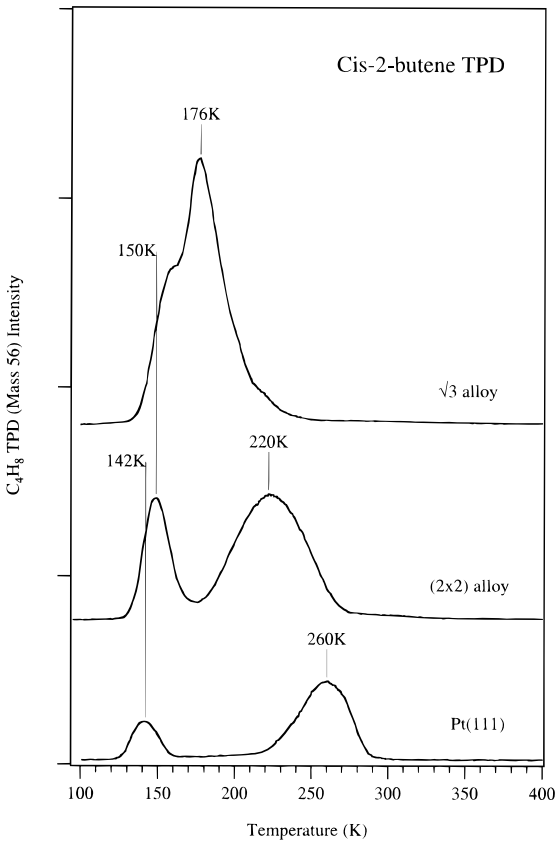

Figure 9. Comparison of the C_4H_8 TPD spectra after 0.71-langmuir *cis*-2-butene exposures on all three surfaces at 95 K to produce a chemisorbed monolayer and some concentration of physisorbed species.

H/molecule in a peak at 302 K and then extensive dehydrogenation of the hydrocarbon fragments that result from butylidyne decomposition in a peak at 384 K in TPD. Slightly lower stability of the butylidyne species formed from *cis*-2-butene compared to 1-butene causes a strong overlap of the first two H_2 desorption states, and this leads to an overestimation of the size of the first peak in Figure 10b. We note that the peak temperatures in the TPD spectra in Figure 10a agree well with those reported previously,[4] but our quantitative analysis of those peak areas disagrees slightly with the former report of 1:6:1 for the three regions defined by the peaks at 294 and 381 K and the range 583−705 K.

Figure 11a provides a summary of the H_2 desorption from the *cis*-2-butene monolayer on all three substrates. Absolutely no H_2 desorption is observed on the $\sqrt{3}$ surface alloy, while about 10% of the amount of the H_2 yield from the Pt(111) surface is desorbed on the (2 × 2) alloy. Several H_2 TPD spectra from *cis*-2-butene exposures on the (2 × 2) alloy at 95 K are reproduced on an expanded scale in Figure 11b. A fairly sharp peak at 400 K and a broad peak centered at 670 K are typical of all the exposures. The H_2 yield from the (2 × 2) alloy corresponds to the decomposition of 6% of the chemisorbed *cis*-2-butene monolayer. The amount of residual carbon detected by AES measurements after the TPD experiments with *cis*-2-butene on both the (2 × 2) and $\sqrt{3}$ alloys was consistent with these results.

No extra spots in LEED were observed in annealing experiments following *cis*-2-butene adsorption on both the (2 × 2) and $\sqrt{3}$ alloys at 95 K, indicating that no adsorbate structures possessing long-range order were formed. The adsorption, desorption, and reaction of *cis*-2-butene on the surface alloys did not change the surface structure; i.e., no detectable changes occurred in the LEED pattern after a TPD experiment.

3.3. Isobutene. The H_2 and C_4H_8 TPD results for isobutene adsorption on Pt(111) and the (2 × 2) and $\sqrt{3}$ surface alloys, including a quantitative analysis of the uptake curve, coverage, and dehydrogenation mechanism on Pt(111) are presented elsewhere.[19] We summarize these results here in order to make comparisons to the other butene isomers. On Pt(111), the isobutene monolayer coverage is 0.12 ML, with 0.065 ML irreversibly adsorbed and 0.055 ML reversibly chemisorbed. Integration of the corrected H_2 TPD spectrum from the isobutene

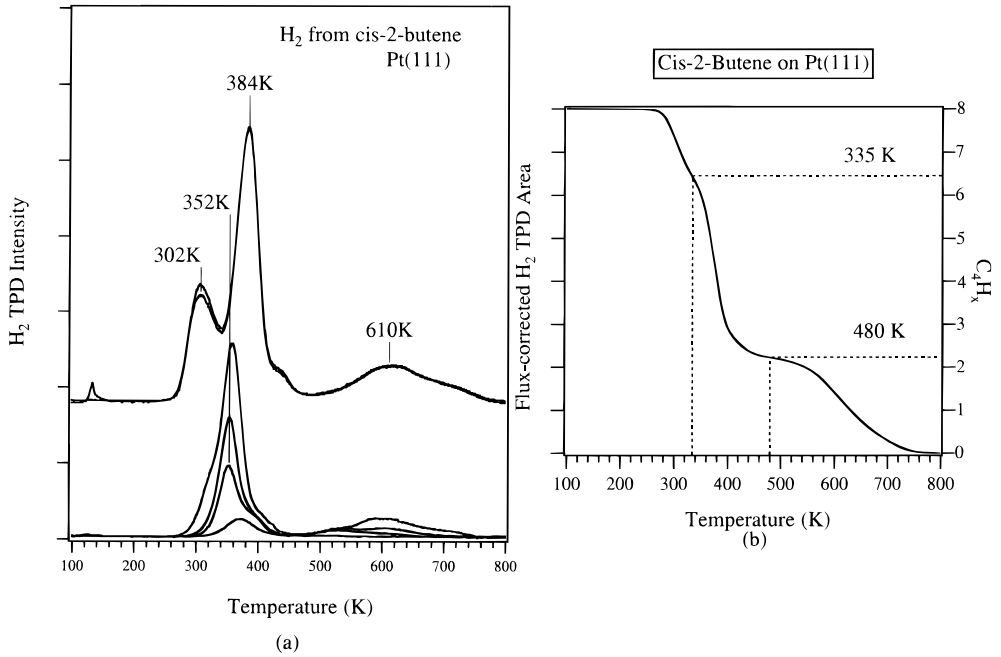

Figure 10. (a) H_2 desorption spectra resulting from *cis*-2-butene decomposition on Pt(111). The exposures were 0.0, 0.06, 0.12, 0.24, 0.48, and 1.1 langmuir of *cis*-2-butene on Pt(111) at 95 K. (b) Surface stoichiometry of hydrocarbon fragments resulting from *cis*-2-butene (C_4H_8) dehydrogenation as a function of temperature on Pt(111).

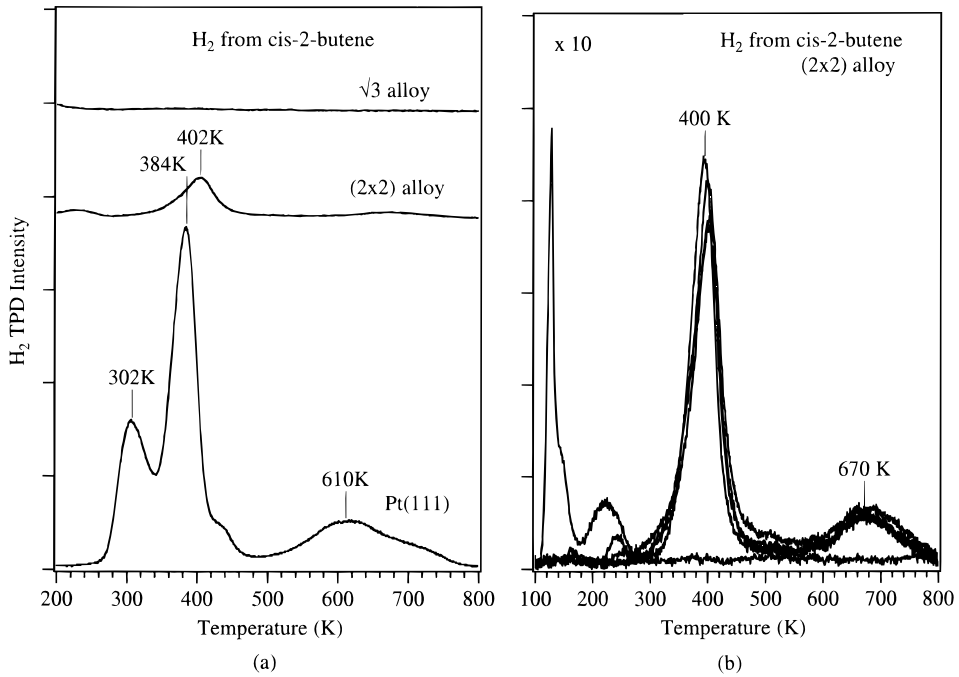

Figure 11. (a) H_2 desorption from *cis*-2-butene decomposition on Pt(111), the (2 × 2) and $\sqrt{3}$ alloy surfaces. (a) H_2 desorption resulting from *cis*-2-butene decomposition on the (2 × 2) alloy. The exposures were 0.0, 0.06, 0.24, and 1.4 langmuir of *cis*-2-butene on the (2 × 2) alloy at 95 K.

monolayer indicates the following dehydrogenation processes:

$$C_4H_8 \xrightarrow{330\ K} C_4H_7 \xrightarrow{400\ K} C_4H_5 \xrightarrow{480\ K} C_4H_3 \xrightarrow{535\ K} C_4H_{1.5}$$

Chemisorbed isobutene on Pt(111) desorbs at 280 K at low coverage and then shifts to 268 K at monolayer coverage. Alloyed Sn decreases the bonding of isobutene to the surface as reflected in the molecular desorption temperatures of 240−212 and 180−170 K on the (2 × 2) and $\sqrt{3}$ alloys, respectively, depending on the coverage. Sn adatoms also strongly suppress isobutene decomposition, as seen in the H_2 TPD yield. Only 3% of the chemisorbed monolayer decomposes on the (2 × 2) alloy to liberate H_2, which corresponds to only 5% of the H_2 yield from isobutene decomposition on Pt(111). No decomposition occurs on the $\sqrt{3}$ alloy. However, the alloyed Sn does not appreciably affect the amount of monolayer coverage compared to that formed on Pt(111) at 95 K. Also, no extra LEED spots in addition to those due to the alloy structures, i.e., either the (2 × 2) or ($\sqrt{3}$ × $\sqrt{3}$)R30° pattern, were observed over a range of substrate temperatures of 95−800 K.

4. Discussion

Adsorption studies for an increasing number of hydrocarbons on these two Pt−Sn surface alloys have now been carried out,

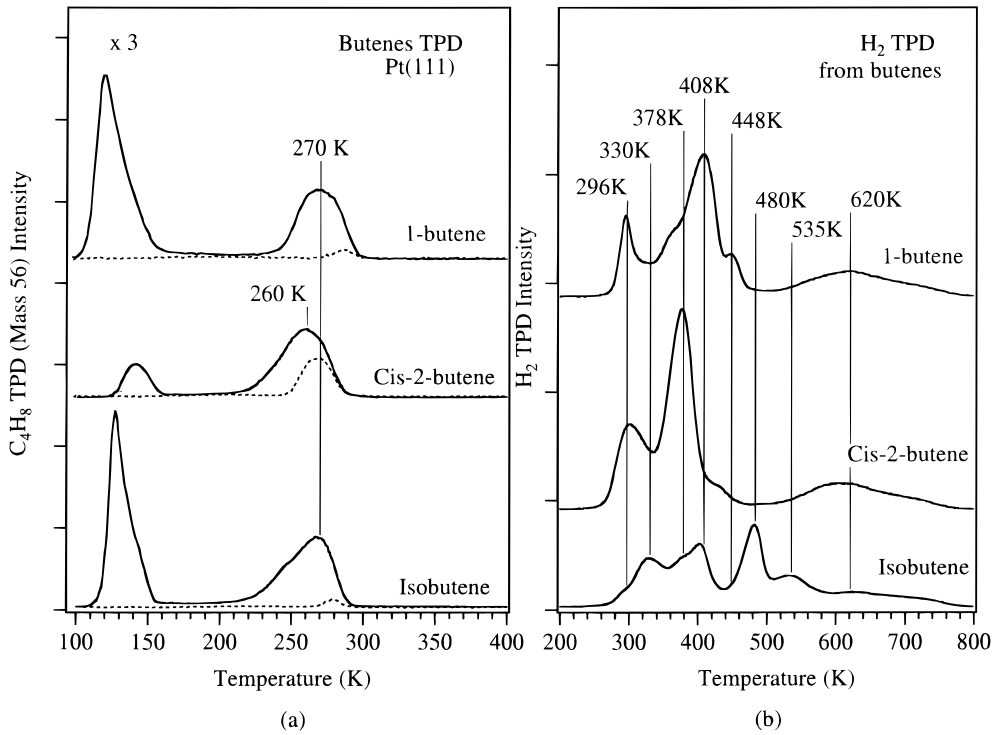

Figure 12. (a) Comparison of the C_4H_8 TPD spectra from coverages of the three butenes slightly larger than one monolayer (solid lines) and low coverage (dashed lines) on Pt(111) after adsorption at 95 K. (b) Comparison of the corresponding H_2 TPD spectra from the three butenes adsorbed on Pt(111).

and some general trends are starting to emerge. The alloys adsorb alkanes (*n*-butane,[1] isobutane,[1] and cyclohexane[29]) reversibly—decomposition under UHV conditions is completely suppressed. The adsorption energies of these saturated hydrocarbons are only slightly reduced by incorporating Sn into the Pt(111) surface, and this reduction is linearly dependent on Sn concentration in the surface. A decrease of about 18% in the adsorption energy of these alkanes occurs on the $(\sqrt{3} \times \sqrt{3})$-R30°Sn/Pt(111) alloy with $\Theta_{Sn} = 0.33$ compared to Pt(111). Alloying Sn in Pt(111) has a similar effect on the adsorption energies of alkenes[19,27,30] if one compares the results on the (2 × 2) alloy with 0.25 ML of Sn atoms, but bonding on the $\sqrt{3}$ alloy is relatively much weaker. Regarding the reactivity of these surfaces, benzene[29] decomposition is completely suppressed on both alloys, but for ethylene,[19,27] propylene,[19] and all of the butene isomers, decomposition is completely suppressed on the $\sqrt{3}$ alloy but not fully eliminated on the (2 × 2) Sn/Pt(111) alloy. Cyclohexene,[30] cyclohexadiene,[31] and acetylene[32] dehydrogenate even on the $\sqrt{3}$ alloy. We now discuss our recent results on the C_4 alkenes, the isomers of butene, in order to continue to develop a better understanding of the general reactivity of these Pt−Sn surface alloys, in particular with regard to olefin chemistry.

4.1. Butene Adsorption and Reaction on Pt(111). Figure 12a shows a comparison of the thermal desorption spectra of butene isomers adsorbed on Pt(111) at 95 K. Since all three of these molecules are di-σ-bonded on Pt(111) at low temperatures,[16] the similarities in the desorption temperature of the most strongly bound chemisorbed state (260−270 K at monolayer coverage) indicate that the chemisorption bond strength is unaffected by the identity of the butene isomer on Pt(111). These values can also be compared to 284 and 272 K for ethylene and propylene desorption on Pt(111), and this reveals only a weak inductive effect to slightly decrease the Pt−C bond strength upon substitution of alkyl groups for H in ethylene. These TPD spectra also reveal another desorption state at about 140 K which is difficult to resolve clearly from the multilayer state near 120 K. The origin of this 140 K peak is not clear, but we currently believe that it is not part of the chemisorbed monolayer principally due to arguments that we can make about the maximum coverage that can be accommodated within the chemisorbed monolayer. No such state for ethylene or propylene was observed, and this also leads one to assign this feature to physisorbed layers.

In Figure 12b, we compare the dehydrogenation of butene isomers on Pt(111). They all form alkylidyne species on Pt(111) by removal of one H per molecule at similar temperatures (260−300 K).[4,8] The stability of these alkylidyne species does not vary much, such that heating above 335 K initiates dehydrogenation of all of the alkylidynes. However, the dehydrogenation mechanism and the overall stoichiometry of the surface hydrocarbon fragments as a function of temperature are different for the butylidyne from isobutene compared to 1-butene and *cis*-2-butene, since the H_2 TPD traces are quite different above 335 K.

One would expect that the reactivity of these butene isomers with Pt(111) would be similar. All of the isomers have relatively weak β-CH, i.e., allylic C−H, bonds in addition to the stronger vinylic C−H bonds[33] that one finds in ethylene, and this leads to a higher reactivity than for ethylene. Since 1-butene has the fewest number of allylic C−H bonds, one might expect a slightly lower reactivity compared to the other isomers, but since cleavage of one of these bonds causes reaction, this may not cause a large effect. The uptake curves showed that 50−60% of the chemisorbed layer decomposed upon heating for each of the butenes. These results can be compared to 44 and 56% for ethylene and propylene, respectively.

Table 1 summarizes all of the coverage values that we have determined: the saturation monolayer coverage (Θ_{sat}), fraction of reversibly (Rev) and irreversibly (Irr) chemisorbed butenes on Pt(111) and the two alloy surfaces, and the saturation monolayer coverage calculated from a closest-packing model (Θ_{cp}). Θ_{cp} is the upper limit for the number of molecules in the chemisorbed monolayer. The butene isomers have very

TABLE 1: Summary of the Coverages of Butene Isomers on Pt(111) and Two Sn/Pt(111) Surface Alloys

	values from uptake curves and TPD measurements				AES (C/Pt) Θ_C
	Pt(111)	(2 × 2) alloy	$\sqrt{3}$ alloy	Θ_{cp}	Irr %, Pt(111)
1-butene	Rev = 53%	Rev = 93%	Rev = 100%		0.39
	Irr = 47%	Irr = 7%			0.39
	Θ_{sat} = 0.17 ML	Θ_{sat} = 0.21 ML	Θ_{sat} = 0.21 ML	Θ_{cp} = 0.23 ML	57%
cis-2-butene	Rev = 37%	Rev = 94%	Rev =100%		0.30
	Irr = 63%	Irr = 6%			0.30
	Θ_{sat} = 0.13 ML	Θ_{sat} = 0.10 ML	Θ_{sat} = 0.10 ML	Θ_{cp} = 0.23 ML	58%
isobutene	Rev = 46%	Rev = 97%	Rev = 100%		0.26
	Irr = 54%	Irr = 3%			0.26
	Θ_{sat} = 0.12 ML	Θ_{sat} = 0.11 ML	Θ_{sat} = 0.14 ML	Θ_{cp} = 0.23 ML	54%

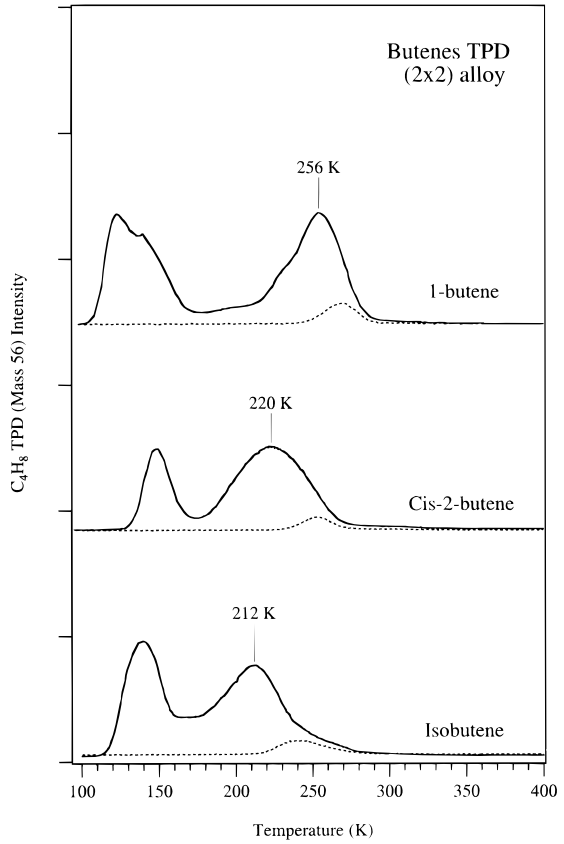

Figure 13. Comparison of C_4H_8 TPD spectra from coverages of the three butenes slightly larger than one monolayer (solid lines) and low coverage (dashed lines) on the (2 × 2) alloy after adsorption at 95 K.

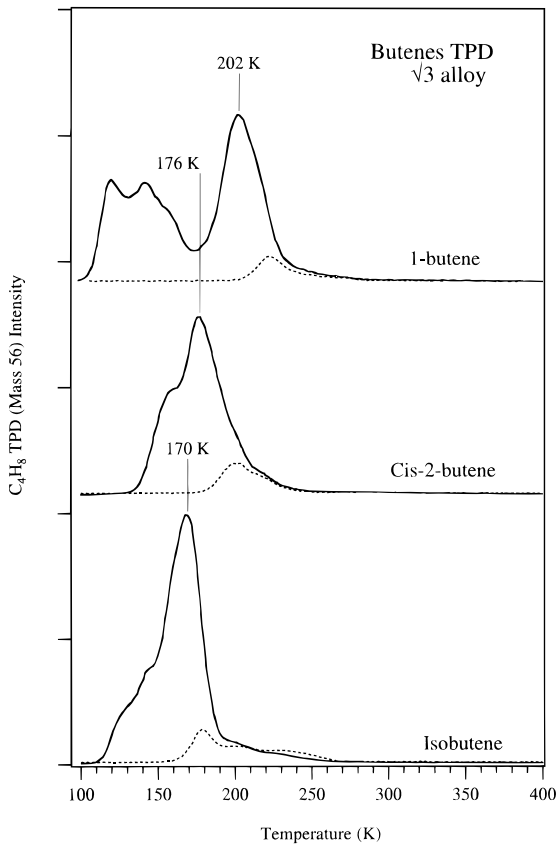

Figure 14. Comparison of the C_4H_8 TPD spectra from coverages of the three butenes slightly larger than one monolayer (solid lines) and low coverage (dashed lines) on the $\sqrt{3}$ alloy after adsorption at 95 K.

similar molecular sizes, and this leads to essentially the same value for Θ_{cp}. We found Θ_{sat} for 1-butene on Pt(111), however, to be appreciably larger than for the other isomers but still significantly smaller than Θ_{cp}. These differences are due to the importance of specific sites and bonding geometries (that are obviously required to form the strongly chemisorbed di-σ-bonded butenes) and the influence of the different molecular geometries on self-site-blocking.

The extent of irreversible adsorption, i.e., the fraction of the chemisorbed monolayer that dehydrogenates to liberate H_2 and leave carbon on the surface after TPD, reported in Table 1 can be calculated in two ways. First, as discussed in the Results section, we have used TPD uptake curves to determine these fractions. Second, the decomposition amount can be obtained from the AES C(272)/Pt(237 eV) peak-to-peak height ratio measured after TPD experiments (heating up to 800 K). Calibration comes from C/Pt = 0.22 corresponding to Θ_C = 0.22 ML due to 44% decomposition of 0.25 ML of C_2H_4 on Pt(111).[27] Assuming that the values for Θ_{sat} are correct and that a linear relationship exists between the C/Pt AES ratio and Θ_C over this small range gives an independent determination of the irreversibly adsorbed fraction of the butenes.

4.2. Butene Adsorption and Reaction on Sn/Pt(111) Surface Alloys. Figures 13 and 14 summarize C_4H_8 desorption following the adsorption of butene isomers on the (2 × 2) and $\sqrt{3}$ alloys, respectively, at 95 K. At monolayer coverage on the (2 × 2) alloy, *cis*-2-butene and isobutene desorb at much lower temperatures than 1-butene, even though the desorption temperatures are similar on Pt(111). If one looks at the lower coverage behavior (Figures 3b and 8b and also shown as dashed line curves in this figure), much of this shift originates in a larger coverage-dependent shift for *cis*-2-butene and isobutene[19] on the (2 × 2) alloy compared to that for 1-butene. The desorption peak from the chemisorbed state of *cis*-2-butene on the (2 × 2) alloy is about 60 K wide, compared to about 40 K for 1-butene and isobutene. This also indicates different interactions within the adlayer, and possibly with the surface, depending on the butene isomer.

In Figure 14, the same trend of the desorption temperatures of the chemisorbed states on the $\sqrt{3}$ alloy is observed with

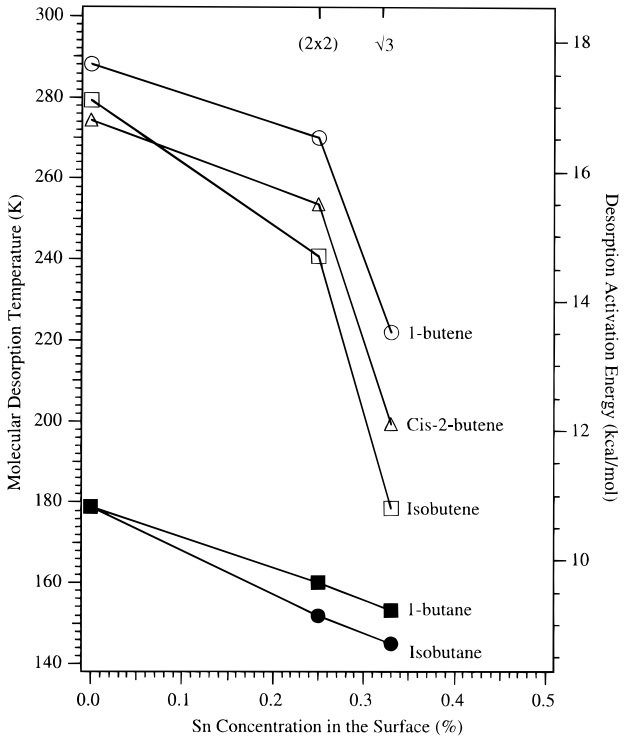

Figure 15. Plot of the molecular desorption peak temperatures for 1-butene, *cis*-2-butene, and isobutene on Pt(111) and the two Sn/Pt-(111) surface alloys vs surface Sn concentration. Also shown for comparison are the molecular desorption peak temperatures for butane and isobutane on these surfaces.[16] The right-hand axis gives an estimate of the corresponding molecular desorption activation energy and adsorption energy.

1-butene higher than *cis*-2-butene and isobutene, as on the (2 × 2) alloy. The highest temperature desorption peaks on the $\sqrt{3}$ alloy were narrower than on the (2 × 2) alloy, although *cis*-2-butene also showed a large coverage-dependent shift on the $\sqrt{3}$ alloy.

Figure 15 summarizes the molecular desorption temperatures of butene isomers, along with values for *n*-butane and isobutane. Peak temperatures at low coverage were used to construct this plot in order to help avoid the influence of lateral interactions in the adlayer. The decrease in desorption temperatures, and concomitant decrease in desorption activation energies (shown on the right-hand axis), for the butenes is not linear with the surface Sn concentration. A relatively larger effect on adsorption energies is observed upon forming the $\sqrt{3}$ alloy. This behavior has been seen for all of the alkenes studied.[19,27,30] This is in contrast to what we have observed for all of the alkanes studied,[1,29] where a linear dependence on the surface Sn concentration was seen. Alkanes form only weak H-bonding or dispersion interactions with the surface, probing the polarizability of the surface and showing only a weak dependence on the surface Sn concentration. UPS spectra of these alloys[34] show only small changes in the Pt valence band due to alloying and a change in the work function. The effect of alloying Sn to form the (2 × 2) alloy on the adsorption energy of the butenes is similar to that for the C_4 alkanes. This must mean that the sites necessary for strong chemisorption are not strongly affected by alloying. However, in changing the surface Sn concentration from 0.25 to 0.33 ML, i.e., changing from the (2 × 2) to $\sqrt{3}$ alloy, a much larger effect occurred on the butenes compared to the butanes. We associate this significant effect as due to the loss of pure Pt 3-fold hollow sites on the $\sqrt{3}$ alloy and their importance in strongly chemisorbing alkenes.

When Sn is alloyed with Pt to form the Pt−Sn ordered surface alloys, the largest effect on the surface chemistry of butene isomers is the strong suppression of decomposition. H_2 desorption in TPD studies is a convenient and accurate monitor of butene decomposition since no other products are observed in TPD (e.g., alkanes) on both substrates. The attenuation of the amount of decomposition is not proportional to the surface Sn concentration over this range of Sn coverages and is in contrast to the effect of Sn on the butene adsorption energy. Replacing 25% of the surface Pt atoms with Sn atoms reduces the H_2 evolution compared to that from Pt(111) to only 14%, 10%, and 5% for 1-butene, *cis*-2-butene, and isobutene, respectively. No H_2 yield was observed on the $\sqrt{3}$ alloy for all of these butenes, and thus, no decomposition occurs. While it is always very difficult to separate site-blocking and electronic effects, the crucial point is probably the nature of the reactive sites on the alloys. No two adjacent pure Pt 3-fold hollow sites exist on the (2 × 2) alloy, and no Pt 3-fold hollow sites at all exist on the $\sqrt{3}$ alloy. These results indicate the importance of two adjacent pure Pt 3-fold hollow sites for the dehydrogenation of butenes on Pt(111). This result can be generalized to many di-σ-bonded alkenes on Pt(111), but cyclohexene[30] must dehydrogenate via an alternate pathway(s).

Even though Sn is considered to be inert for chemisorption of butenes, the amount of chemisorbed butenes after alloying with either 0.25 or 0.33 ML of Sn is not reduced compared to Pt(111). This shows that the adsorption ensemble requirement for chemisorption of butenes on Pt(111) and the (2 × 2) and $\sqrt{3}$ alloys is at most 4−5, and probably 2−3, Pt atoms. In fact, the same or higher monolayer coverage of butenes chemisorbed on the two Pt−Sn surface alloys is obtained compared to that on Pt(111) at 95 K. This is probably due to a small relaxation of the bonding geometry/site requirements that result from slightly weaker bonding interactions between the butenes and the alloy surfaces.

As a final comment, we point out several implications of these results for the catalytic dehydrogenation of isobutane to isobutene over supported Pt−Sn bimetallic catalysts. Lok et al.[35−37] studied the kinetics and mechanism of the dehydrogenation of isobutane to isobutene over Pt/Al_2O_3 catalysts, both with and without promoters such as Cu, Se, Pb, Ge, In, and Sn. They found that the reaction rate increased for catalysts containing promoters in the order given above, with $Pt-Sn/Al_2O_3$ having the highest rate. Rate increases of up to a factor of 40−70 were observed. They explained their results and the action of promoters in this process according to a decrease in inhibition by the reaction product, an increased reactivity of the coke (due to an alteration of the properties and composition of the coke formed, mainly by an enrichment in the hydrogen stoichiometry), and an increase in the rate of the slow step in the catalytic mechanism—the dissociative adsorption of isobutane. To the extent that the Pt−Sn alloy phases studied here resemble those catalytically active sites on a working catalyst, we can predict an improved performance of Pt−Sn bimetallic catalysts over Pt catalysts. The origin of this effect comes from two features of the Pt−Sn surface alloys. First, decreased isobutene dehydrogenation activity on the Pt−Sn surface alloys increases the selectivity for gas-phase isobutene production and increases the catalyst lifetime by reducing the carbon buildup (coking) that gradually poisons the catalyst surface. Second, a weaker isobutene chemisorption bond provides a shorter lifetime on the surface so that nonselective competing reactions are inhibited while increasing the catalytic reaction rate under conditions were isobutene desorption is reaction-rate-limiting. In previous studies, we also observe a decreased adsorption

energy of *n*-butane and isobutane on these alloy surfaces.[1] However, the decrease in adsorption energy of isobutene compared to isobutane is much larger on the $\sqrt{3}$ alloy, so selectivity can be improved. A final determination of the impact of this work on Pt−Sn catalysis awaits high-pressure reaction studies of the catalytic dehydrogenation of isobutane to isobutene over those well-defined Pt−Sn alloys. Similar studies have been carried out by Paffett and Logan[38] on butane hydrogenolysis on these surfaces.

5. Conclusions

The isomers of butene (1-butene, *cis*-2-butene, and isobutene) have a similar chemisorption bond strength and reactivity on Pt(111). They all are di-σ-bonded in the molecularly chemisorbed state and 50−60% of the chemisorbed monolayer dehydrogenated to form butylidynes below room temperature. Alloying Sn with Pt(111) to form the (2×2) Sn/Pt(111) alloy, with 25% surface Sn, or the $(\sqrt{3} \times \sqrt{3})$R30°Sn/Pt(111) alloy, with 33% surface Sn, has strong effects on the reactivity of butene isomers and a smaller effect on the butene adsorption energies. For all of the butene isomers, the irreversibly adsorbed fraction of the chemisorbed monolayer decreases to less than 7% on the (2×2) alloy, and no decomposition occurs on the $\sqrt{3}$ alloy. This is due in part to the decreased adsorption energy of the butenes on the alloys, since desorption and dehydrogenation are competitive reactions, but the main effect is to increase the barrier for C−H bond scission due to site blocking by Sn since no two adjacent pure Pt 3-fold sites exist on the (2×2) alloy and no pure Pt 3-fold sites at all exist on the $\sqrt{3}$ alloy. The alloyed Sn weakens the chemisorption bond of the butenes on the two surface alloys compared to Pt(111), from about 17 to 15−16 kcal/mol on the (2×2) alloy and 11 to 13.5 kcal/mol on the $\sqrt{3}$ alloy. The relatively large effect on the adsorption energy when comparing the (2×2) and $\sqrt{3}$ alloys is due to the elimination of pure Pt 3-fold sites on the $\sqrt{3}$ alloy, and the importance of these sites in strongly bonding alkenes. The monolayer coverages for the butenes are 0.17, 0.13, and 0.12 ML for 1-butene, *cis*-2-butene, and isobutene on Pt(111), respectively. These monolayer coverages are unaffected, or even slightly higher, by the presence of surface Sn at these Sn concentrations. This indicates that only small ensembles of a few Pt atoms are required to chemisorb butenes. Our results comparing the surface chemistry of the butenes and butanes on these Pt−Sn surface alloys are consistent with the observed effects of adding Sn to supported Pt catalysts used for isobutane dehydrogenation. Thus, Pt−Sn alloy phases may be important to the function of these catalysts.

Acknowledgment. This work was supported by the U.S. Department of Energy, Office of Basic Energy Sciences, Chemical Sciences Division. We also thank Dr. Chen Xu for early contributions to this work.

References and Notes

(1) Xu, C.; Koel, B. E.; Paffett, M. T. *Langmuir* **1994**, *10*, 166.
(2) Paffett, M. T.; Gebhard, S. G.; Windham, R. G.; Koel, B. E. *J. Phys. Chem.* **1990**, *94*, 6831.
(3) Kesmodel, L. L.; Dubois, L. H.; Somorjai, G. A. *J. Chem. Phys.* **1979**, *70*, 2180.
(4) Salmeron, M.; Somorjai, G. A. *J. Phys. Chem.* **1982**, *86*, 341.
(5) Creighton, J. R.; White, J. M. *Surf. Sci.* **1983**, *129*, 327.
(6) Koestner, R. J.; Van Hove, M. A.; Somorjai, G. A. *J. Phys. Chem.* **1983**, *87*, 203.
(7) Horsley, J. A.; Stohr, J.; Koestner, R. J. *J. Chem. Phys.* **1985**, *83*, 3146.
(8) Avery, N. R.; Sheppard, N. *Proc. R. Soc. London, Ser. A* **1986**, *A405*, 1.
(9) Malik, I. J.; Brubaker, M. E.; Mohsin, S. B.; Trenary, M. *J. Chem. Phys.* **1987**, *87*, 5554.
(10) Land, T. A.; Michely, T.; Behm, R. J.; Hemminger, J. C.; Comsa, G. *J. Chem. Phys.* **1992**, *97*, 6774.
(11) Cremer, P.; Stanners, C.; Niemantsverdriet, J. W.; Shen, Y. R.; Somorjai, G. *Surf. Sci.* **1995**, *328*, 111.
(12) Cassuto, A.; Mane, M.; Tourillon, G.; Parent, P.; Jupille, J. *Surf. Sci.* **1993**, *287/288*, 460.
(13) Koestner, R. J.; Frost, J. C.; Stair, P. C.; Van Hove, M. A.; Somorjai, G. A. *Surf. Sci.* **1982**, *116*, 85.
(14) Ogle, K. M.; Creighton, J. R.; Akhter, S.; White, J. M. *Surf. Sci.* **1986**, *169*, 246.
(15) Anderson, A. B.; Kang, D. B.; Kim, Y. *J. Am. Chem. Soc.* **1984**, *106*, 6597.
(16) Cassuto, A.; Tourillon, G. *Surf. Sci.* **1994**, *307*−*309*, 65.
(17) Bertolini, J. C.; Cassuto, A.; Jugent, Y.; Massardier, J.; Tardy, B.; Tourillon, G. *Surf. Sci.* **1996**, *349*, 88.
(18) Windham, R. G.; Bartram, M. E.; Koel, B. E. *J. Phys. Chem.* **1988**, *92*, 2862.
(19) Tsai, Y.-L.; Xu, C.; Koel, B. E. *Surf. Sci.*, submitted.
(20) Jiang, L. Q.; Koel, B. E. *J. Phys. Chem.* **1992**, *96*, 8694.
(21) Paffett, M. T.; Windham, R. G. *Surf. Sci.* **1989**, *208*, 34.
(22) Overbury, S. H.; Mullins, D. R.; Paffett, M. T.; Koel, B. E. *Surf. Sci.* **1991**, *254*, 45.
(23) Atrei, A.; Bardi, U.; Rovida, G.; Torrini, M.; Zanazzi, E.; Ross, P. N. *Phys. Rev.* **1992**, *B46*, 1649.
(24) Galeotti, M.; Atrei, A.; Bardi, U.; Rovida, G.; Torrini, M. *Surf. Sci.* **1994**, *313*, 349.
(25) Throughout this paper, we have tacitly assumed that no isomerization occurs during molecular adsorption and desorption of these butenes. We did not distinguish the different isomers in our current mass spectroscopy results. While NEXAFS and UPS results have shown that no isomerization occurs during the adsorption process for the butenes,[16] it has not been established that no isomerization occurs during desorption.
(26) Redhead, P. A. *Vacuum* **1962**, *12*, 203.
(27) Paffett, M. T.; Gebhard, S. C.; Windham, R. G.; Koel, B. E. *Surf. Sci.* **1989**, *223*, 449.
(28) Busse, H.; Voss, M. R.; Koel, B. E. To be published.
(29) Xu, C.; Tsai, Y.-L.; Koel, B. E. *J. Phys. Chem.* **1994**, *98*, 585.
(30) Xu, C.; Koel, B. E. *Surf. Sci.* **1994**, *304*, 249.
(31) Peck, J. W.; Koel, B. E. *J. Am. Chem. Soc.* **1996**, *118*, 2708.
(32) Xu, C.; Peck, J. W.; Koel, B. E. *J. Am. Chem. Soc.* **1993**, *115*, 751.
(33) In the gas phase, the C−H bond dissociation energy, D_{300}(C−H), for the vinylic hydrogen in ethylene is 111.2 kcal/mol, while D_{300}(C−H) = 88.8 kcal/mol for the allylic hydrogen in propylene.[39]
(34) Xu, C.; Koel, B. E. *Surf. Sci.* Lett. **1994**, *304*, L505.
(35) Lok, L. K.; Gaidai, N. A.; Gudkov, B. S.; Kiperman, S. L.; Kogan, S. B. N. D. Zelinskii Institute of Organic Chemistry, Academy of Sciences of the USSR, Moscow. Plenum: New York, 1987; p 1184. Translated from *Kinet. Katal.* **1986**, *27*, 1365.
(36) Lok, L. C.; Gaidai, N. A.; Kiperman, S. L. N. D. Zelinskii Institute of Organic Chemistry, Academy of Sciences of the USSR, Moscow. Plenum: New York, 1987; p 1112. Translated from: *Kinet. Katal.* **1986**, *27*, 1275.
(37) Lock, L. C.; Gaidai, N. A.; Gudkov, B. S.; Kostyukovskii, M. M.; Kiperman, S. L.; Podkletnova, N. M.; Kogan, S. B.; Bursian, N. R. N. D. Zelinskii Institute of Organic Chemistry, Academy of Sciences of the USSR, Moscow. Plenum: New York, 1987; p 1190. Translated from: *Kinet. Katal.* **1986**, *27*, 1371.
(38) Szanyi, J.; Anderson, S.; Paffett, M. T. *J. Catal.* **1994**, *149*, 438.
(39) Berkowitz, J.; Ellison, G. B.; Gutman, D. *J. Phys. Chem.* **1994**, *98*, 2744.